Characterization of Right-Handed and Left-Handed Shapes

Yaacov Hel-Or[*]   Shmuel Peleg   David Avnir[†]

Department of Computer Science
The Hebrew University of Jerusalem
91904 Jerusalem, ISRAEL

Abstract

Many natural shapes are chiral (or handed). Our hands, for example, have a right-hand version and a left-hand version, the two types being mirror images of each other. Molecules are also classified according to their chirality, which determines their chemical characteristics. Glucose, for example, is sweet only in one chirality, while it is tasteless in the other.

The notion of chirality for two dimensional binary shapes is studied, and scales for quantitative assessment of the degree of shape-chirality are developed. The chirality measures are based on boundary analysis, and perfom well on shapes with natural variations, scaling differences or digitization errors. The measures can also be used with partially occluded shapes, and provide indications on the change of chirality as resolution changes.

1 Introduction

A planar object is *chiral* in 2D if and only if it does not have a symmetry axis in the 2D plane. A right hand will never be similar to a left hand unless we look at one of them through a mirror. Thus, the set of all human hands can be divided into two classes, each having its own specific chirality.

Not only body parts have right or left handedness. This property, *chirality*, exists almost everywhere. Chirality has special significance in the study of elementary particles [3] whose

---

[*]Y.H. was supported by the Leibniz Center for Research in Computer Science.

[†]Dept. of Organic Chemistry.

chirality is due to their spin. Similarly, molecules can appear in two possible configurations, called D (dextro) chirality and L (levo) chirality [6], each having different chemical characteristics. For instance, glucose of D-chirality is sweet, whereas glucose of L-chirality is tasteless. The first to observe the importance of chirality in chemistry were the French chemists Louis Pasteur (1822-1895) and Jean Baptiste Biot (1774-1862) who determined the connection between the chirality of crystals and the deflection of the plane of polarization light passing through them [2].

The goal of our work is to examine a set of two dimensional shapes, and conclude whether the objects in the set are chiral. Once shapes are found to be chiral, we would like to classify them according to chirality class. Theoretically, it is enough to check whether an object has a reflective symmetry, because chirality is a form of asymmetry. However, almost no real object is exactly symmetric (especially after digitization), and therefore we must determine whether the lack of symmetry is a dominant characteristic of the object.

Figure 1 exhibits some intuitive properties of this analysis. Shape A_1 is symmetric and non-chiral since its mirror image, A_2, can be superimposed on it after translation and rotation. Shape B_1, which is obtained by shortening one arm of A_1, is chiral. Shape C_1, with an even shorter arm, is chiral to a greater degree than B_1. Shortening the arm completely to produce the straight line D_1 results in a symmetric shape again. This paper develops a method which quantifies chirality, and could compute by how much is shape C_1 more chiral than shape B_1.

2   Basic Definitions

2.1   Chirality

Let K be a set of points in $\Re^2$, and let $R_\ell(K)$ be the set formed after reflecting K about the line ℓ in $\Re^2$. K will be called *chiral* if and only if $R_\ell(K) \neq K$ for all ℓ. Put simply, K is chiral if and only if it can not be superimposed on its mirror image. It can be shown that if K is not chiral then the line ℓ, which satisfies $R_\ell(K) = K$, passes through the centroid of K.

Let K be a chiral set, and let $R_\ell(K) = \hat{K}$, that is $\hat{K}$ is the mirror image of K. K and $\hat{K}$ are called *enantiomers* and cannot be superimposed on each other.
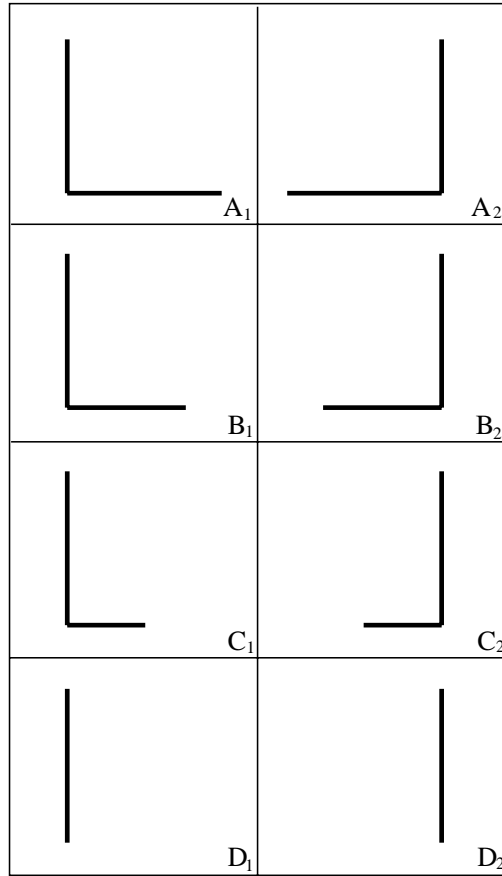
Figure 1: The shapes in the right column are mirror images of the shapes in the left column. Shape A_1 is non-chiral, since it can be superimposed on its mirror image, A_2, using only translations and rotations. B_1 is chiral, C_1 even more chiral and D_1 is symmetric.

2.2   Symmetry

- K is *symmetric* if and only if there exists an isometry (a distance preserving transformation) which is not the identity, that transforms K onto itself. Therefore, a set which is not chiral is symmetric.

- K is *asymmetric* if and only if there is no isometry that transforms K onto itself.

- K is *dissymmetric* if and only if there is no reflection that transforms K onto itself.

Note: A set is chiral if and only if it is asymmetric or at least dissymmetric. There are shapes, like the shape of the letter Z, that are symmetric, dissymmetric and chiral.

3

3 Chirality Measures

Implementing the mathematical definition of chirality is not practical since most natural shapes are not exactly symmetric, and even shapes with exact symmetry will lose this property after digitization. We have tried to quantify chirality using moment invariants [5] and the correlation between a shape and its mirror image, but have found such measures to be too sensitive to noise and to variations caused by digitization. Furthermore, such analysis could not distinguish between enantiomers. Another possible approach is to decompose the image into a sum of chiral basis functions, like the polar Fourier transform presented by Bigün and Granlund [1]. We have tried such an approach, and found it also to be sensitive to small and irrelevant variations. Furthermore, the conversion into polar coordinates of a grid-sampled image introduced additional inaccuracies.

We have found a chirality measure based on rotational features of the body to be the most practical. As clockwise rotation of an object is identical to counterclockwise rotation of its mirror image, non-chiral objects, which are identical to their mirror-image, will exhibit indifference to the direction of rotation. Chiral objects, on the other hand, will behave differently for the two directions of rotation.

In our scheme we use the following idea. Imagine the object as rotating in a medium full of tiny particles. Some boundary segments will "collect" particles, and pull them towards the axis of rotation. We will use the length of these segments as a feature for chirality analysis. A spiral as shown in Figure 2, for example, will have no "collecting" points when rotating clockwise. Its leading edge will push particles away from the axis of rotation. In counter-clockwise rotation, however, the leading edge of the spiral will be "collecting", and pulling particles towards the axis of rotation. We will initially analyze rotations around the centroid, but eventually will use other points. The choice of the center of rotation will be discussed later in this paper.

3.1 Boundary Based Measures

Let K be the set of points (pixels) of a simply connected 2D object. Let $E = \{e_i\}_{i=1}^{n}$ be the set of edge pixels of K, $E \subseteq K$. The edge pixels $\{e_i\}$ are ordered by following the border [9] in the direction such that the object is always on the right as in Figure 3.

4

Figure 2: In clockwise rotation, particles will be pushed away from the center of the spiral. In counter-clockwise rotation, particles will be "collected", or pulled in, by all points on the leading edge of the spiral.
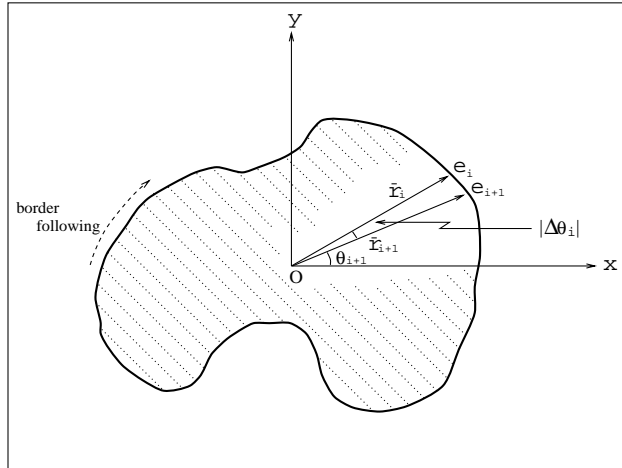

Figure 3: Illustration of the definitions on boundary pixels.

For a boundary pixel e_i and an axis of rotation O we define the following:

- $\vec{r_i}$: the vector from O to e_i.

- d_i : the length of $\vec{r_i}$.

- θ_i : the angle between $\vec{r_i}$ and the x-axis, represented in the range $-\pi < \theta_i \leq \pi$.

- Δd_i : $d_{(i+1)\,mod\,n} - d_i$.

- $\Delta\theta_i$: $\theta_{(i+1)\,mod\,n} - \theta_i$.   This is the angle (e_i, O, e_{i+1}), represented in the range $-\pi < \Delta\theta_i \leq \pi$.

5

Figure 3 illustrates some of these definitions. When dealing with noisy images, the following averages can be used: $\Delta d_i = (d_{i+1} - d_{i-1})/2$ and $\Delta \theta_i = (\theta_{i+1} - \theta_{i-1})/2$.

A boundary segment between e_i and e_{i+1} will encounter particles upon clockwise rotation, only if $\Delta d_i < 0$ (Figures 4.C, 4.D). It will encounter particles in counter-clockwise rotation if $\Delta d_i > 0$ (Figures 4.A, 4.B). Particles encountered by a leading edge will be pushed away unless the edge pulls them in when $\Delta \theta_i > 0$ (Figures 4.A, 4.C).
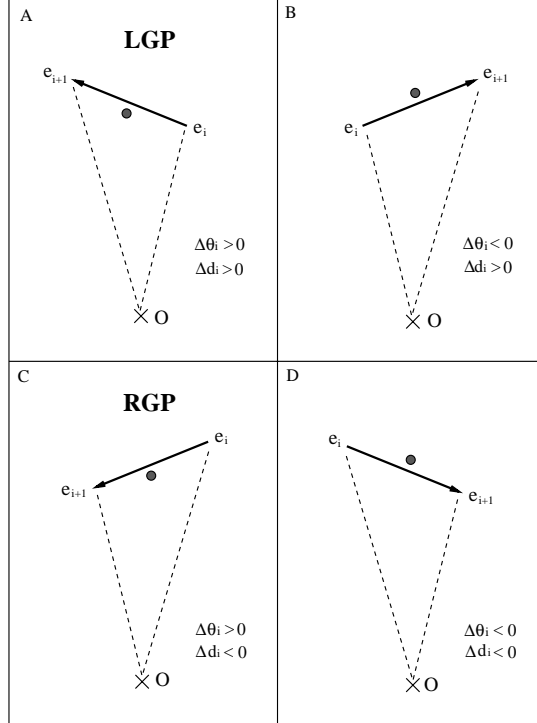

Figure 4: Properties of edge segments in rotation.
A, B) Edge segments encountering particles in counter-clockwise rotation.
C, D) Edge segments encountering particles in clockwise rotation.
A) Edge segments encountering and grasping particles in counter-clockwise rotation (LGP).
C) Edge segments encountering and grasping particles in clockwise rotation (RGP).

Denote the subsets of edge segments E that collect particles upon clockwise and counter-clockwise rotation by RGP (right-grasp-pixels) and LGP (left-grasp-pixels), respectively. RGP or LGP are defined as follows, and illustrated in Figure 4.

$$
\begin{aligned}
LGP &= \{e_i | \Delta \theta_i > 0 \ , \ \Delta d_i > 0\} \\
RGP &= \{e_i | \Delta \theta_i > 0 \ , \ \Delta d_i < 0\} \ .
\end{aligned}
\tag{1}
$$

6

Note that $RGP \cap LGP = \emptyset$, and $LGP \cup RGP \subseteq E$. In practice we do not use only the signs of $\Delta\theta_i$ and Δd_i as in Definition (1), since the sign can be very unstable for values near zero. Therefore, thresholds ε_1 and ε_2 are chosen to give the following definition:

$$
\begin{aligned}
LGP &= \{e_i | \Delta\theta_i > \varepsilon_1/d_i \ , \ \Delta d_i > \varepsilon_2\} \\
RGP &= \{e_i | \Delta\theta_i > \varepsilon_1/d_i \ , \ \Delta d_i < \varepsilon_2\} .
\end{aligned}
\tag{2}
$$

As a chirality measure we then use the normalized difference

$$
Z = \frac{|LGP| - |RGP|}{|E|},
\tag{3}
$$

where $|LGP|$ represents the number of pixels in the set LGP. The normalization by the number of edge points $|E|$ makes the chirality measure independent of object size, but dependent on the ratio of grasp-pixels to edge-pixels. The measure Z has the following properties:

1. If left and right rotations have the same number of grasp pixels then $Z = 0$.

2. As the absolute value of Z increases, so does the degree of chirality of the analyzed object.

3. The sign of Z is an indicator for the absolute configuration. $Z > 0$ indicates left-handed chirality (more particles are collected upon a left hand rotation than upon a right hand rotation). $Z < 0$ indicates right handed chirality.

In order to further refine the chirality measurement we use the paradigm of torque, which is force multiplied by the distance from the axis. Following this paradigm we get a slightly different chirality measure. Let

$$
L = \frac{1}{d_{max}} \sum_{i \in LGP} d_i \ ,
$$

and

$$
R = \frac{1}{d_{max}} \sum_{i \in RGP} d_i \ .
$$

7

Figure 5: Application of the two rotational chirality measures on several shapes. The thick edges represent RGP pixels and the double edges represent LGP pixels. The computed measures are summarized below.

object	Measure (3)	Measure (4)	object	Measure (3)	Measure (4)
A1	0.02	0.88	C1	-0.04	-0.25
A2	-0.02	-0.80	C2	-0.01	0.23
B1	0.26	0.94	D1	0.10	0.97
B2	-0.27	-0.97	D2	-0.16	-1.00

To avoid scale effects, d_{max}, the maximal value of d_i, is taken as a normalization parameter. The chirality measure will be defined as

$$Z' = \frac{L - R}{L + R} \quad . \tag{4}$$

This measure is analogous to the total normalized torque that is exerted on the axis by the collected particles. Figure 5 shows measures (3) and (4) applied to several shapes, when the centroid is used as the axis of rotation. Note that the shape in Figure 5.c is chiral, but since $|LGP| = |RGP|$ Measure (3) fails to find its chirality, while Measure (4) succeeds. By applying Measure (3) to the shapes of Figure 1, we obtain the predicted results which are shown in Figure 6. In Figure 6, shapes (a) and (d) are not chiral, and indeed have minimum chirality measure. Shapes (b) and (c) are both chiral, and (c) is more chiral than (b). These properties re also reflected in the computed measurements.
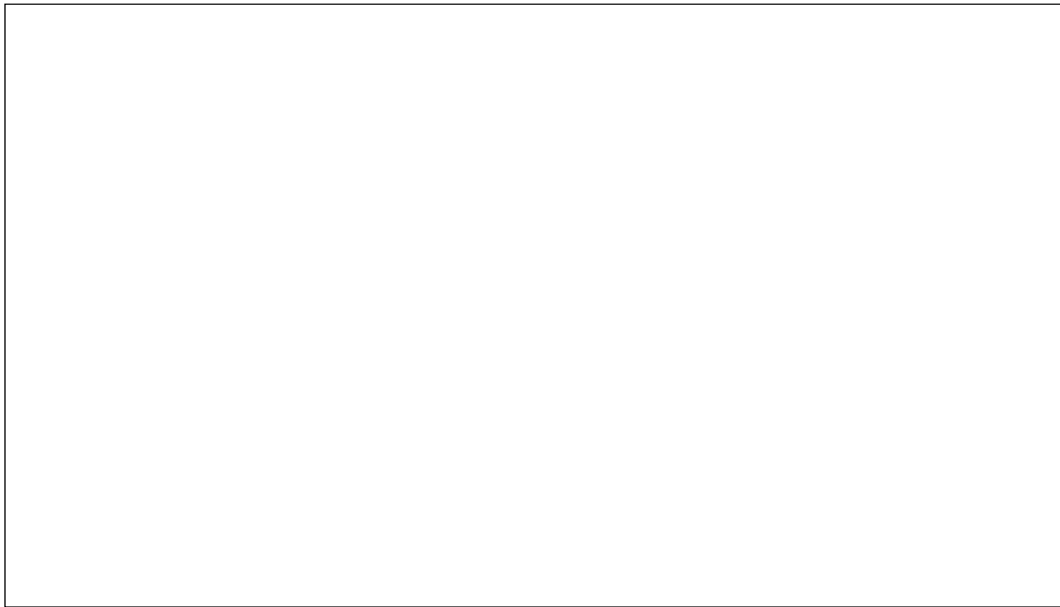

Figure 6: Application of Measure (3) to the shapes of Figure 1. Rotation is around the centroid. The computed measures are summarized in the table below.

object	Measure (3)	object	Measure (3)
a	-0.001584	c	-0.006369
b	-0.005445	d	0.0

9

4 Center of Chirality

Any chirality measure depends on the choice of the axis of rotation. The centroid has initially been used as an axis of rotation, but this choice can be misleading in some cases, especially for partially occluded shapes. Even for spirals the centroid is not the center of the spiral, as shown in Figure 7. We therefore define the following: the *center of chirality* is a point that maximizes the rotational chirality measure (the absolute values of Measure (3)) when used as a rotation axis. Figure 7 shows the center of chirality for two shapes. It finds the correct center of the spiral, as well as the correct center of another partially occluded shape. The stability of the center of chirality in the cases of partially occluded shapes is an important feature, as it is hard to assure that all analyzed shapes will be entirely visible.
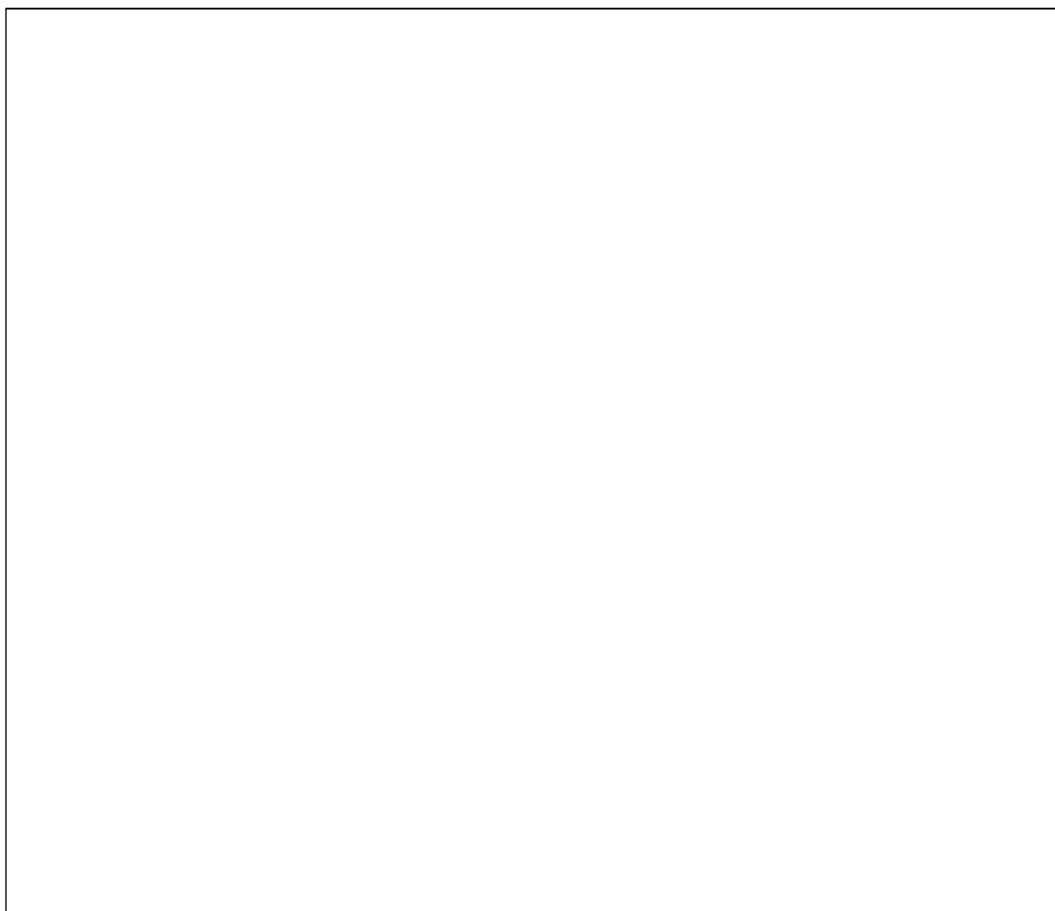

Figure 7: The center of chirality (right) and centroid (left) of two shapes. For spirals (bottom) the center of chirality better corresponds to the center of the spiral than the centroid.

10

Computing the center of chirality for an image involves the computation of chirality measure many times, each time with another pixel as the rotation axis, and then choosing the pixel which maximizes this measure. In order to reduce this high computational complexity and to avoid computing the chirality measure around every point of the image, several heuristics can be used. We could, for example, start searching for the maximal chirality at the centroid, examine a small neighborhood of the current location, and move on to the pixel of highest chirality in this neighborhood. This iterative search will stop when a point has higher chirality measure than all its neighbors. Simulated Annealing [7] can be used to prevent stopping at local maxima, but is not computationally efficient. A faster method to reach the center of chirality uses a multiresolution search.

4.1 Multiresolution Search

Define a pyramid [8] as a sequence of reduced resolution images. The lowest level of the pyramid, L_0, will be the original image whose side length is 2^N. L_1 will be a reduced image, having a side length of 2^{N-1}, etc. There are several methods for reducing L_i to L_{i+1}; the simplest is when every pixel of L_{i+1} is an average of a 2×2 block in L_i. For binary shapes as discussed in this paper, a pixel of L_{i+1} will get the majority value of the relevant 2×2 block in L_i. The pyramid, multiresolution structure can be used to speed up the computation and to measure resolution-dependent chirality information.

The computation of the center of chirality in the pyramid is very fast. We start by computing the center of chirality at a small image using exhaustive search. This is fast, as the small image has only a small number of pixels. Let e_i be the center of chirality at pyramid level i. The center of chirality at level $i-1$ can now be computed by projecting e_i into level L_{i-1}, and searching for maximum chirality only in a small neighborhood around this projection. This speed-up is correct when details added between levels L_i and L_{i-1} change the location of the center of chirality only by a limited distance.

Computing the chirality measure at all resolution levels not only speeds up computation, but reveals additional information on the shape under consideration. The chirality at lower resolution levels describes a feature of the general shape, while chirality at higher resolution levels incorporates the features of the fine details. When the chirality of the fine details differs from the chirality of the general shape, the chirality measure can change drastically with resolution as shown in Figure 8.a .

The pyramid can also help in the analysis of non-connected objects. The rotational

chirality measures works only on simply connected objects. When fragmented objects are analyzed, the reduction of resolution can yield connected objects at lower resolution level, where analysis is possible. Figure 8.b shows the analysis of non-connected object at lower resolution.
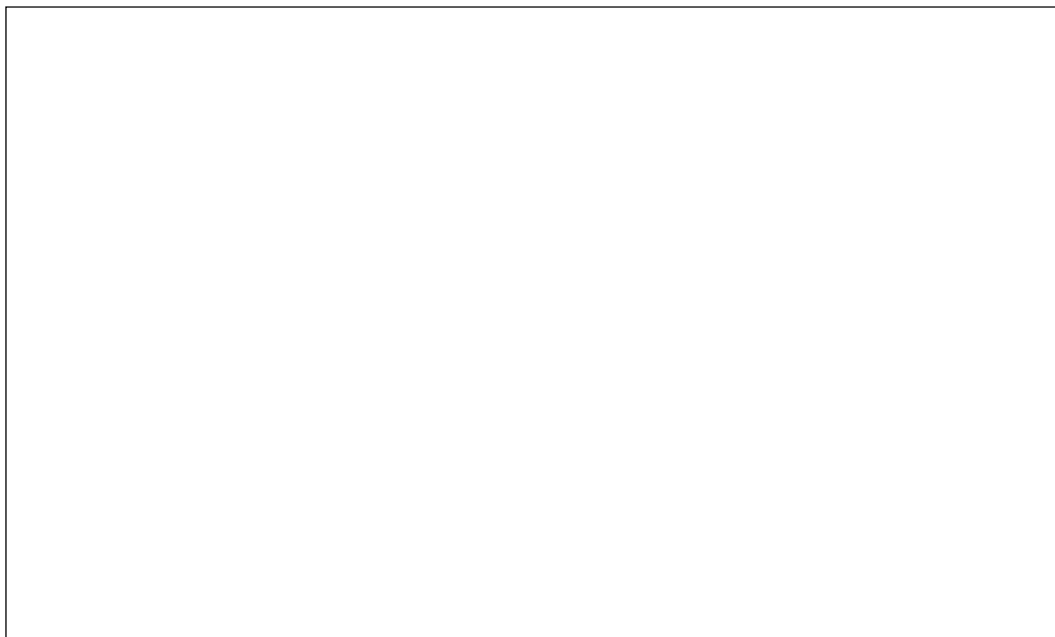

Figure 8: Multiresolution Chirality Analysis. a) Different chirality for general shape at low resolution and details at high resolution. b) Non-connected object that becomes connected at lower resolution level.

5 Chemistry Application

Chirality has special significance in the study of chemistry and in particular in field of surface science, which deals with adsorbed molecules. A 3D mulecule loses one degree of freedom when adsorbed onto a surface; therefore it can be treated as a 2D object, and the conditions for chirality are significantly relaxed. It should be noted that chirality is by far more common in the adsorbed (2D) state, compared to the bulk (3D) state. Consider for example n-butane (Figure 9.1-2). This is a non-chiral molecule in 3D, yet when adsorbed it becomes chiral. We have applied our chirality measure to some 2D molecules represented by a sticks representation, with results presented in Figure 9.

No.			No.		
1			5		
2			6		
3			7		
4			8		

Figure 9: The molecules' skeleton structures analyzed using Measure (4) (see table below). The rotation centers are chosen to be the centroids, and are indicated by crosses.

No.	molecule	Measure (4)	No.	Molecule	measure (4)
1	R-n-butane	+0.98	5	2-methylhexane	−0.06
2	S-n-butane	−0.98	6	3-ethylpentane	−0.96
3	propane	−0.05	7	3-methylhexane	+0.43
4	n-hexane	+0.36	8	2-methylbutane	−0.48

The rotational chirality measure helped us to develop a new sense of chirality called *dynamic chirality*, which is described in [4]. Although not stated explicitly, the concept of chirality is a static concept; a molecule is judged to be chiral or non-chiral based on its static shape. This static concept collapses if one substitutes the static picture with a dynamic one. Moreover, a moving object can be chiral even if its static shape is non-chiral. A rotating molecule will therefore be judged to be dynamic-chiral or not by applying the measure with the origin at the center of rotation of the molecule. Figure 10 demonstrates how dynamic chirality is determined by the choice of rotational center. This chirality map shows the degree of chirality as a function of the rotation axis.
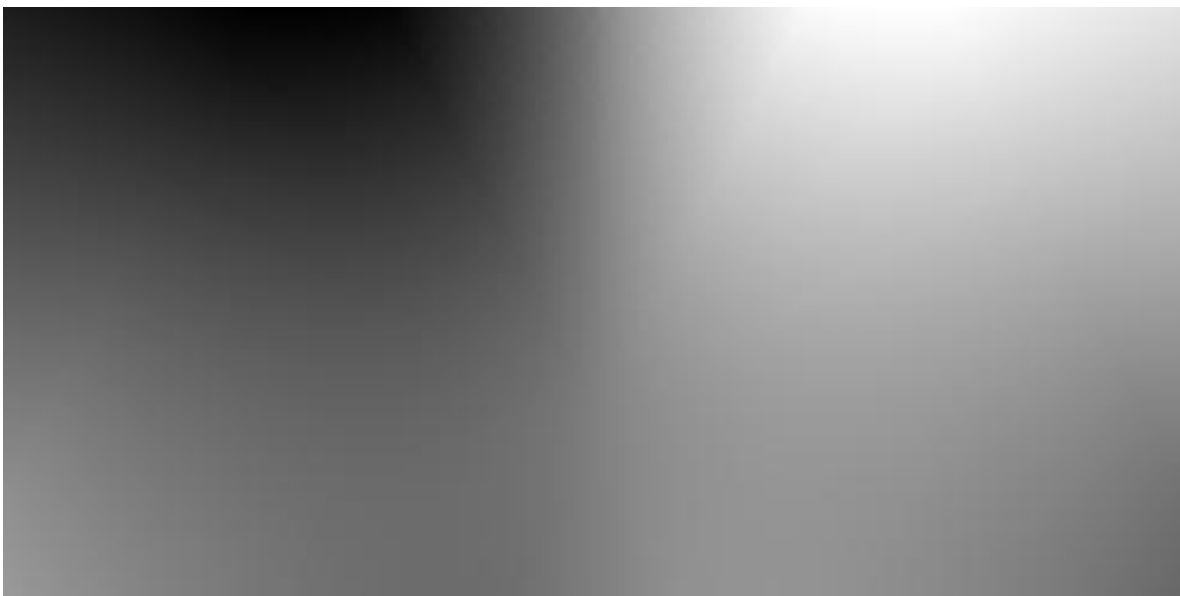
Figure 10: A grey-level map of the degree of chirality as a function of location of the rotation axis. White represents highest positive chirality value, and black represents lowest negative chirality values. The chirality was computed according to measure (4).

6 Concluding Remarks

A measure based on rotational features of two dimensional objects has been suggested for chirality analysis of binary simply-connected shapes. This measure is robust, and is immune to insignificant deviation and some occlusions.

References

[1] J. Bigün and G.H. Granlund. Central symmetry modelling. In *Third European Signal Processing Conference*, pages 883–886, The Hague, September 1986.

[2] R. Dubos. *Pasteur and Modern Science*. Wiley, Anchor, 1960.

[3] M.B. Green. Superstrings. *Scientific American*, pages 44–56, September 1986.

[4] Y. Hel-Or, S. Peleg, and D. Avnir. Two dimensional rotational dynamic chirality and a chirality scale. *Langmuir*, in press.

[5] M. Hu. Visual pattern recognition by moment invariants. *IRE Trans. on Information Theory*, pages 179–187, 1962.

[6] H.H. Jaffe and M. Orchin. *Symmetry in Chemistry*. Wiley, New York, 1965.

[7] S. Kirpatrick, C.D. Gellat, Jr., and M.P. Vecchi. Optimization by simulated annealing. *Science*, pages 671–680, May 1983.

[8] A. Rosenfeld. *Multiresolution Image Processing and Analysis*. Springer-Verlag, 1984.

[9] A. Rosenfeld and A.C. Kak. *Digital Picture Processing*, volume 2. Academic Press, New York, 1982.